

# Correlation function for the Grid-Poisson Euclidean matching on a line and on a circle

Elena Boniolo

*Dipartimento di Fisica dell'Università degli Studi di Milano,  
via Celoria 16, I-20133 Milano, ITALY  
elena.boniolo@gmail.com*

Sergio Caracciolo

*Dipartimento di Fisica dell'Università degli Studi di Milano, and INFN,  
via Celoria 16, I-20133 Milano, ITALY  
Sergio.Caracciolo@mi.infn.it*

Andrea Sportiello

*LIPN, and CNRS, Université Paris 13, Sorbonne Paris Cité,  
99 Av. J.-B. Clément, 93430 Villetaneuse, FRANCE  
Andrea.Sportiello@lipn.fr*

December 3, 2024

## Abstract

We compute the two-point correlation function for spin configurations which are obtained by solving the matching problem of points on grid with points chosen at random when the cost depends on their distance. We provide the analytical solution in the continuum in some particular case and check it numerically by looking at the critical problem on the finite size.

# 1 Introduction

Let us consider the complete bipartite graph  $\mathcal{K}_{N,M}$ , whose set of vertices  $V$  is partitioned in  $V = \mathcal{R} \cup \mathcal{B}$ . We shall call *red* the set of vertices  $\mathcal{R} = \{r_1, \dots, r_N\}$  of cardinality  $|\mathcal{R}| = N$  and *blue* the other set  $\mathcal{B} = \{b_1, \dots, b_M\}$  of cardinality  $|\mathcal{B}| = M$ . We are interested in the set  $\Pi$  of maximal matchings on  $\mathcal{K}_{N,M}$ , that is injective mappings  $\{\pi : \mathcal{R} \rightarrow \mathcal{B}\}$  if  $N < M$ , otherwise  $\{\pi : \mathcal{B} \rightarrow \mathcal{R}\}$ . Given a weight  $w(r_i, b_j) = w(i, j) \in \mathbb{R}^+$  to each edge, we assign a cost to each maximal matching  $\pi \in \Pi$

$$E(\pi) = \begin{cases} \sum_{i=1}^N w(i, \pi(i)) & \text{when } N < M ; \\ \sum_{j=1}^M w(\pi(j), j) & \text{when } M < N . \end{cases} \quad (1)$$

The *optimal* matching is the maximal matching that realizes the minimum cost

$$E_{opt} = E(\pi_{opt}) = \min_{\pi \in \Pi} E(\pi) . \quad (2)$$

This problem models a variety of concrete applications in optimisation theory. In particular, it is the discrete version of a problem introduced by Monge [1], back in 1781, where blue and red sites did correspond to production and exploitation sites of some resource, and the matching is optimising the cost of transportation. The continuous version of the problem, in which one has to find the mapping which minimises the transport condition between two given measures (the red and the blue ones) is also of relevance and is studied under the name of Monge-Kantorovič problem [2].

The research of the optimal matching in a bipartite weighted graph is usually called the *assignment problem*. From the point of view of computational complexity theory this is a polynomial problem, in the sense that there are algorithms able to produce the solution which requires, even in the worst case, a number of elementary steps bounded by a polynomial in the number of degrees of freedom of the problem. A classical algorithm for the assignment problem which finds an optimal matching in worst-case polynomial time is due to H. Kuhn [3], who called it *Hungarian Algorithm* as a tribute to the country of origin of the authors of the two main lemmas on which it is based, Kőnig and Egerváry. As reported by Knuth [4], after the work of Munkres [5] for speeding up the recovering procedure, the polynomial is cubic in the number of degrees of freedom.

More interesting questions can be asked in the more general case in which the weights on the graph become stochastic variables. In particular, we are motivated to consider these problems because of the close connection between random optimization problems and the statistical mechanics of disordered systems [6–10]. Indeed, when the weights  $w(i, j)$  are equally distributed random variables, by using the celebrated *replica trick*, Mezárd and Parisi could compute the average cost

for both the matching on the complete graph [11], the *random matching problem*, as on the complete bipartite graph [12], the *random bipartite matching problem*. See [13] for a derivation without replicas.

The model we are going to discuss is the *Grid-Poisson matching problem* in the box  $\Lambda = [0, L]^d \subset \mathbb{R}^d$  with integer  $L$ . The red vertex set  $\mathcal{R}$  is chosen to be the set of points in the hypercubic lattice  $\mathbb{Z}^d$  with semi-integer coordinates which are also in  $\Lambda$ , so that  $N = L^d$ . The blue vertex set  $\mathcal{B}$  is a set of  $M$  points chosen at random in  $\Lambda$ . The weight is taken to be the Euclidean distance  $d(i, j)$  between  $r_i$  and  $b_j$ , or also

$$w(i, j) = d^p(i, j) \quad (3)$$

with a generic  $p$ .

A related model, the *Poisson-Poisson matching problem*, where both the red and blue sets occur as independent Poisson processes of equal intensity, has been considered in [14–16]. The *Euclidean monopartite matching problem* has also been studied by using the replica trick [12], by taking corrections to the random matching problem. The *minimax Grid-Poisson matching problem* has been studied in [18, 19]. In this problem for each maximal matching only the largest contribution from an edge to the cost is taken into account. Then the chosen matching is the one where this largest contribution is minimal. Remark that this solution is achieved by taking the limit of infinitely large exponent  $p$  in the weights (3).

In the limiting cases  $N \ll M$  and  $M \ll N$  the matching is very simple, because each point is associated with its nearest neighbour. Only when  $N \sim M$  we expect long-range correlations of the order of the size of the system. We shall look at the *continuum* limit in which both  $N$  and  $M$  become infinitely large by keeping fixed the ratio

$$\rho := \frac{M}{N}. \quad (4)$$

We also expect that the involution in which  $N$  and  $M$  are exchanged gives rise essentially to the same problem: the algorithm which solves the problem is the same. Therefore we easily predict that the critical point is the self-dual point where  $M = N$ , that is  $\rho = 1$ . Therefore we shall set

$$t := \rho - 1 \quad (5)$$

so that the critical point is exactly at the value of the *reduced temperature*  $t = 0$ .

Our aim is to study the correlations which emerge in the *scaling region* around the critical point.

Let  $r_i$ , with  $i = 1, \dots, N$  be the vector of integer coordinates for the red points and  $b_j$ , with  $j = 1, \dots, M$ , the vector of real coordinates for the blue points, then let

$$\varphi_i := \begin{cases} b_{\pi_{opt}(i)} - r_i & \text{when } M > N, \text{ for } i = 1, \dots, N \\ b_i - r_{\pi_{opt}(i)} & \text{when } N > M, \text{ for } i = 1, \dots, M \end{cases} \quad (6)$$

be the  $i$ -th vector in  $\mathbb{R}^d$  that, in the solution, goes from a red point to the associated blue point. Then

$$E_{opt} = \sum_{i=1}^{\min(N,M)} |\varphi_i|^p \quad (7)$$

and we also introduce, for  $i = 1, \dots, \min(N, M)$ , a spin variable in the sphere  $\mathcal{S}^{d-1}$

$$\sigma_i := \frac{\varphi_i}{|\varphi_i|} \quad (8)$$

that we can associate with the solution. Indeed, we believe that the long-range correlations are associated with these spin variables and not with the length of the vector. Therefore we recover a spin configuration  $\sigma$  for each solution on our grid, with an induced probability  $p(\sigma)$ . In the case  $N > M$  vacancies will also be present. We shall characterize the critical behaviour of our model by looking at the correlation function

$$G(x, y) := \sum_{\sigma} \sigma_x \cdot \sigma_y = \langle \sigma_x \cdot \sigma_y \rangle \quad (9)$$

with  $x, y \in \{0, \dots, L-1\}^d + (1/2, 1/2, \dots, 1/2)$ . When at the point  $x$  there is a vacancy the corresponding spin variable is not defined.

In this paper we will study the simple one-dimensional case in two variants. The first case is with open boundary conditions, that is the box  $\Lambda$  is a line segment. The second one is with periodic boundary condition, where  $\Lambda$  becomes a circle.

Because our solution is on a grid,  $N = L$  and we can study, for all  $r \in \{0, \dots, L\}$

$$G(r; L, t) = \frac{\sum'_{(x,y):d(x,y)=r} G(x, y)}{\sum'_{(x,y):d(x,y)=r} 1} \quad (10)$$

where the sum  $\sum'$  is restricted to all couples of sites for which the correlation function  $G(x, y)$  is well defined. Of course, in the Poisson-Poisson matching problem also the distances between the red points are random variables and, therefore, such a simple function is not easily available.

In the region near criticality we expect *finite-size scaling* of the correlation functions. In particular for the two-point function in (10), this means that it must be a homogeneous function of its arguments, according to

$$G(r; L, t) = L^\alpha F\left(\frac{r}{L}, t L^{\frac{1}{\nu}}\right) \quad (11)$$

where the exponents  $\alpha$  and  $\nu$  and the function  $F$  are *universal*, that is are common to other models in the same universality class. They will be in the following the main argument of our interest.

## 2 Open boundary conditions

Let us start from the case with open boundary conditions.

We first discuss the consequence of the choice of the exponent  $p$  which appears in the weights (3). Take two red points and the two blue points with which they match. There are 24 possible orderings of these 4 points on the line, but we don't distinguish between the two red points and the two blue points so that they become 6. We can concentrate on 3 cases, the others are obtained by exchanging red with blue points.

**First case:** two red points followed by two blue points. Let their positions be, respectively,  $z, z + y, z + y + x_1, z + y + x_2$  with  $x_2 > x_1$ . As the distances are invariant under translations we can choose  $z = 0$  and we can also set  $y = 1$ , by choosing the unit of lengths. Let  $T_1$  be the cost of the matching in which the first red point goes with the first blue one and  $T_2$  the cost of the other possible matching. We shall call the first matching *ordered*. The cost of the matching indicated above and in Fig. 1 are respectively

$$T_1 = (1 + x_1)^p + x_2^p \quad (12)$$

$$T_2 = (1 + x_2)^p + x_1^p. \quad (13)$$

Now,  $T_1 \leq T_2$  if and only if

$$(1 + x_1)^p - x_1^p \leq (1 + x_2)^p - x_2^p \quad (14)$$

but the function  $(1 + x)^p - x^p$  is always increasing, respectively decreasing, when  $p > 1$ , respectively  $p < 1$ . In conclusion, for  $p > 1$  the *ordered* matching has a lower cost. For  $p = 1$  the two matchings have the same cost. For  $p < 1$  the matching with lower cost is the second one. Please note that if we draw the matching with arcs in the second matching the arcs can be drawn with no crossings. This kind of matching are called *non-crossing*.

**Second case:** a red followed by a blue, a red and a blue point. Let the positions be  $0, 1 - x_1, 1, 1 + x_2$  with  $x_1 < 1$ . Remark that the two possible matchings are both *non-crossing*. Let  $T_1$  be always the cost of the *ordered* matching. The costs are now

$$T_1 = (1 - x_1)^p + x_2^p \quad (15)$$

$$T_2 = (1 + x_2)^p + x_1^p. \quad (16)$$

Now,  $T_1 \leq T_2$  if and only if

$$(1 - x_1)^p - x_1^p \leq (1 + x_2)^p - x_2^p. \quad (17)$$

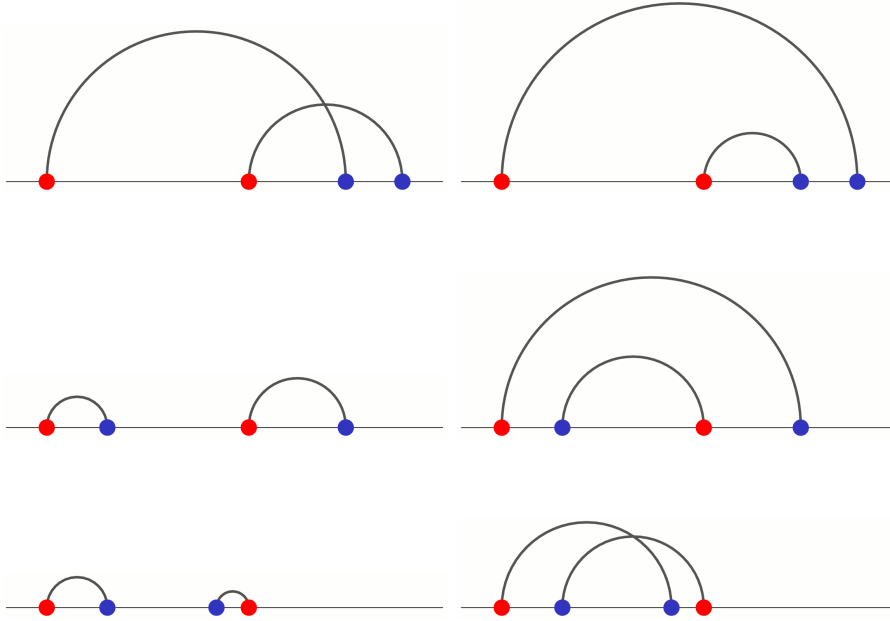


Figure 1: Matchings for size-2 instances. Each line corresponds to a particular disposition of the blue points. The matchings on the left are all *ordered*. The first and the last matching are *crossing*.

For  $p \geq 1$  it is always true, because

$$(1 - x_1)^p - x_1^p \leq 1 \leq (1 + x_2)^p - x_2^p \quad (18)$$

which means that the *ordered* matching has a lower cost. For  $p < 1$ , at fixed  $x_2$ , only for some values of  $x_1$  the *ordered* matching has a lower cost. For example, let  $p = 1/2$  and set  $z = \sqrt{1 + x_2} - \sqrt{x_2}$ , so that  $0 \leq z \leq 1$ . Then if

$$x_1 > \frac{1}{2} \left( 1 - \sqrt{2z^2 - z^4} \right) \quad (19)$$

the *ordered* matching has a lower cost. This is always the case for  $x_1 > 1/2$ .

**Third case:** a red followed by two blue points before the last red one. Let the positions be  $0, x_1, x_2, 1$  with  $x_1 < x_2 < 1$ . In this case the *ordered* matching is *non-crossing*, but the other is *crossing*. The costs are now

$$T_1 = x_1^p + (1 - x_2)^p \quad (20)$$

$$T_2 = x_2^p + (1 - x_1)^p . \quad (21)$$

Now,  $T_1 \leq T_2$  if and only if

$$x_1^p - (1 - x_1)^p \leq x_2^p - (1 - x_2)^p \quad (22)$$

which is always the case for  $p \geq 0$  because then the function  $x^p - (1 - x)^p$  is increasing.

**Proposition 2.1** *For  $M = N$  and  $p > 1$  the optimal matching is ordered.*

**Proof.** We simply note that if the matching is not the *ordered* one there are at least two red points which don't match the blue points in an ordered way. By ordering them we recover a lower cost.  $\square$

Similarly we prove the following:

**Proposition 2.2** *For  $M = N$  and  $p < 1$  the optimal matching is non-crossing.*

First, let us remark that when  $N = M$ , that is where we expect criticality, and when  $p > 1$ , the solution of the matching problem is very simple because there is only one *ordered* matching. Since we are on a line we can label both sets  $\mathcal{R}$  and  $\mathcal{B}$  in increasing order. The solution of the matching problem is the one in which the  $n$ -th red point is associated with the  $n$ -th blue point. Then

$$\varphi_i = b_i - r_i \tag{23}$$

and

$$\sigma_i = \text{sgn } \varphi_i \in \{-1, 1\} \tag{24}$$

is the Ising spin variable that we can associate with the solution.

When  $p = 1$ , it is far from exceptional to meet with situations in which two or more matchings have the same energy, that is, to have degenerate instances. Indeed, we have seen that, in the first case we examined, the crossing and non crossing matching have the same cost.

Whenever  $p > 1$  we shall take  $p = 2$  as our preferential case because, as we shall see in the following, we are able in this case to have exact predictions also in the case of periodic boundary conditions.

## 2.1 Numerical results

We begin from the case  $p = 2$ .

In Fig. 2 we report the correlation function  $G(r; L, t)$  for various choices of the parameter  $t$  when the size of the system has  $L = 6000$ . Each curve is the mean over  $10^3$  instances for the positions of the blue points. Of course, the shape of the function does not change under the transformation  $t \rightarrow -t$ . Then, we notice that  $G(r; L, t)$  presents two ranges of behaviour. If  $|t| < \bar{t}(L)$  (with  $\bar{t}(L) \approx 0.01$  when  $L = 6000$ ) the function is strictly positive, it is decreasing with  $r$ , and has, therefore, a minimum at  $r = L$ . On the other hand, if  $|t| > \bar{t}(L)$ , the shape is

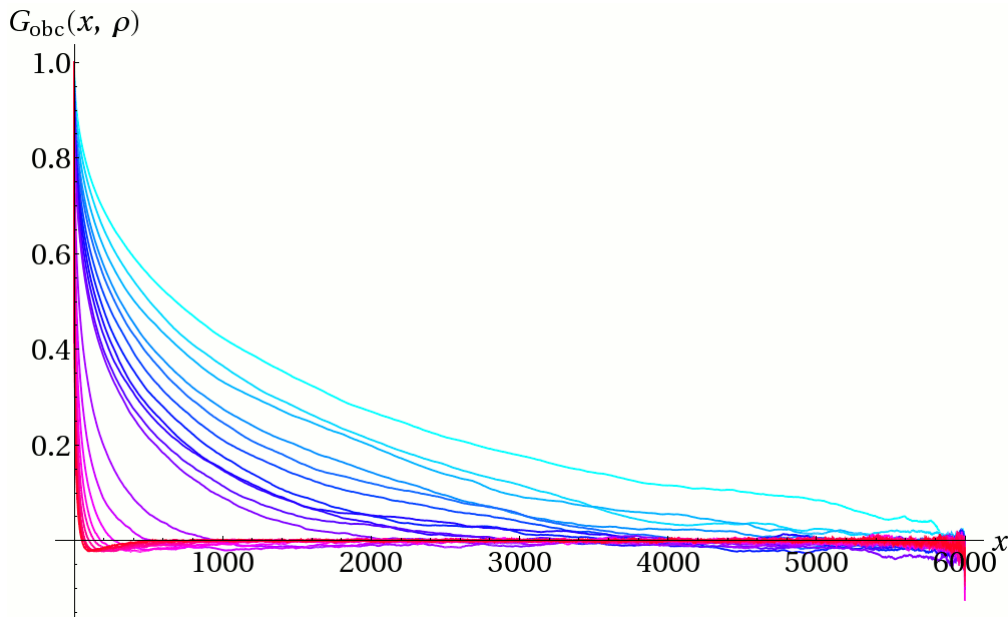


Figure 2: The correlation function with open boundary conditions at size 6000. From cyan to purple,  $t = 0, 0.001, 0.002, 0.003, 0.004, 0.005, 0.006, 0.007, 0.008, 0.009, 0.01, 0.02, 0.03, 0.04, 0.05, 0.06, 0.07, 0.08, 0.09, 0.1$ .

different. It reaches a minimum at an intermediate value  $r'$ , then goes up again approaching zero as  $r \rightarrow L$ . Whenever finite-size scaling holds for the two-point function (11), for large  $L$ , we get that  $\bar{t}(L)L^{\frac{1}{\nu}}$  is constant.

In Fig. 3 we show the correlation functions at criticality for various sizes. In this case each numerical point has been obtained by using  $10^4$  instances for the positions of the blue points. All curves are trivially mapped one onto the others by the simple rescaling  $r \rightarrow r/L$ . That is

$$G(r; L, 0) = \hat{G}\left(\frac{r}{L}\right). \quad (25)$$

This means that in (11) we can set  $\alpha = 0$ .

In order to estimate the exponent  $\nu$ , notice that, if in the scaling region, that is  $|t| < \bar{t}(L)$ , the relation (11) holds, then

$$I(r, L) = L^{-\alpha} \int_0^{\bar{t}(L)} G(r; L, t) dt = L^{-\frac{1}{\nu}} \int_0^{\bar{t}(L)L^{\frac{1}{\nu}}} F\left(\frac{r}{L}, z\right) dz \quad (26)$$

$$\approx L^{-\frac{1}{\nu}} \int_0^{\infty} F\left(\frac{r}{L}, z\right) dz \quad (27)$$

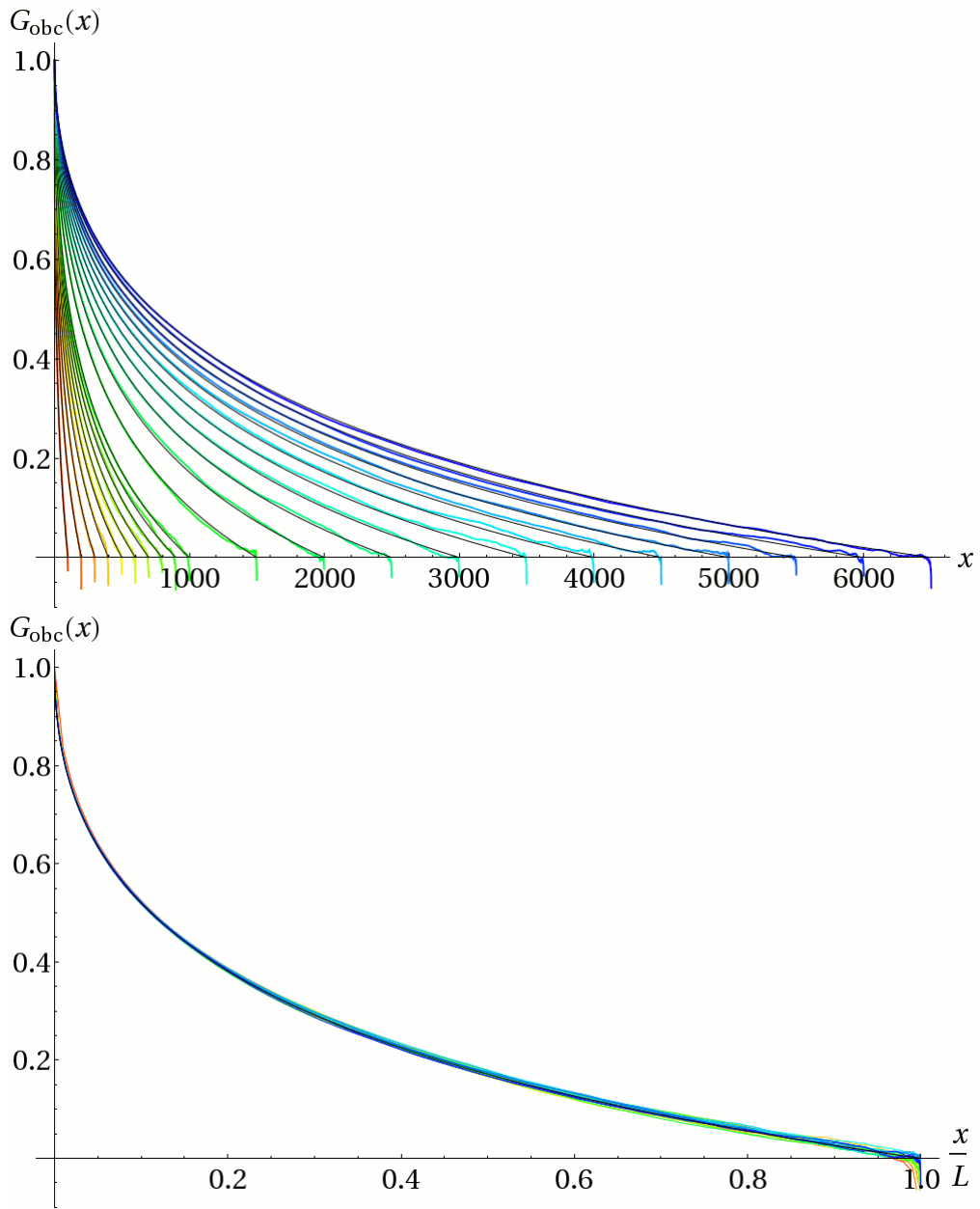


Figure 3: The correlation function at the critical point with open boundary conditions. Top: increasing sizes are represented from red ( $L = 100$ ) to blue ( $L = 6500$ ); Bottom: the same experimental curves, rescaled to show the agreement with the theoretical function, regardless of the size.

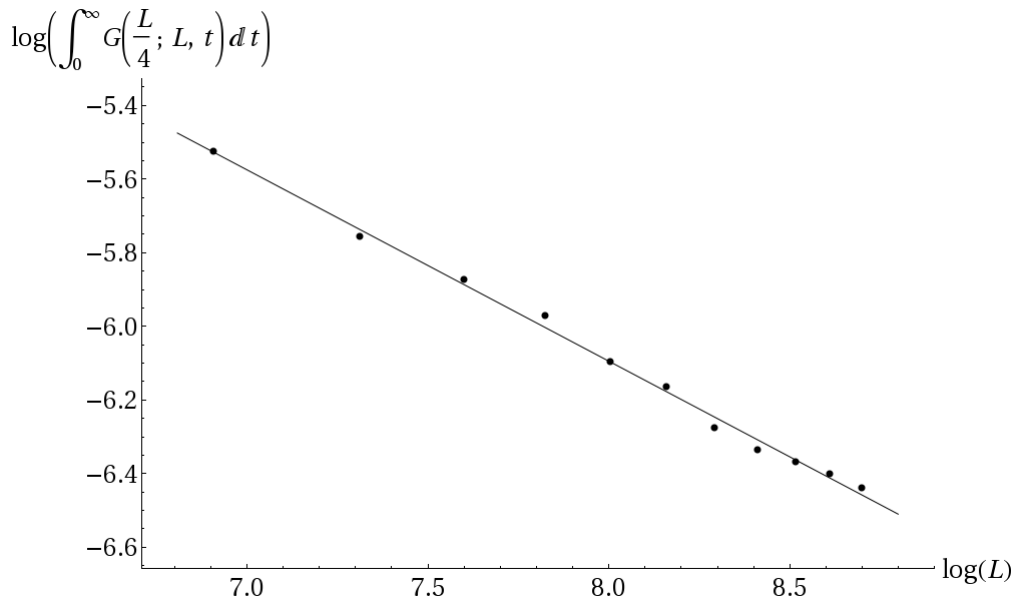


Figure 4:  $\log I(L/4, L)$ , defined by (26), for different values of  $L$ .

because  $F$  vanishes rapidly with increasing  $z$ . As at fixed  $r/L$  the integral of  $F$  simply provides a constant, this expression shows a dependence on  $L$  which determines  $\nu$ .

In Fig. 4 we report the evaluation of  $\log I(r, L)$ , defined by (26), for different values of  $L$  at the point in which  $r = L/4$ . The integral has been evaluated after a polynomial interpolation in  $t$  among the numerical values we had determined. We find

$$\nu = 1.95 \pm 0.05 \quad (28)$$

In Fig. 5 we plot the correlation function at  $r = L/4$  as a function of  $\sqrt{L}t$ . All the points obtained from different values of  $L$ , large enough, and  $t$ , in the scaling region, fall, approximately, on the same curve.

We have performed similar analysis for the case  $p < 1$ , where, in contrast to the case  $p > 1$  there is no reason to expect that the values of the critical indices do not depend on  $p$ . Indeed, while we find always the same exponent  $\nu$ , the exponent  $\alpha$  shows the differences summarised in Table 1.  $\alpha$  has been computed by using the value of the two-point correlation function at distance  $r = L/4$  and the scaling ansatz (11) at criticality. We find approximately

$$\alpha \approx -2(1 - p) \quad (29)$$

in the region  $p \in [0.75, 1]$ .

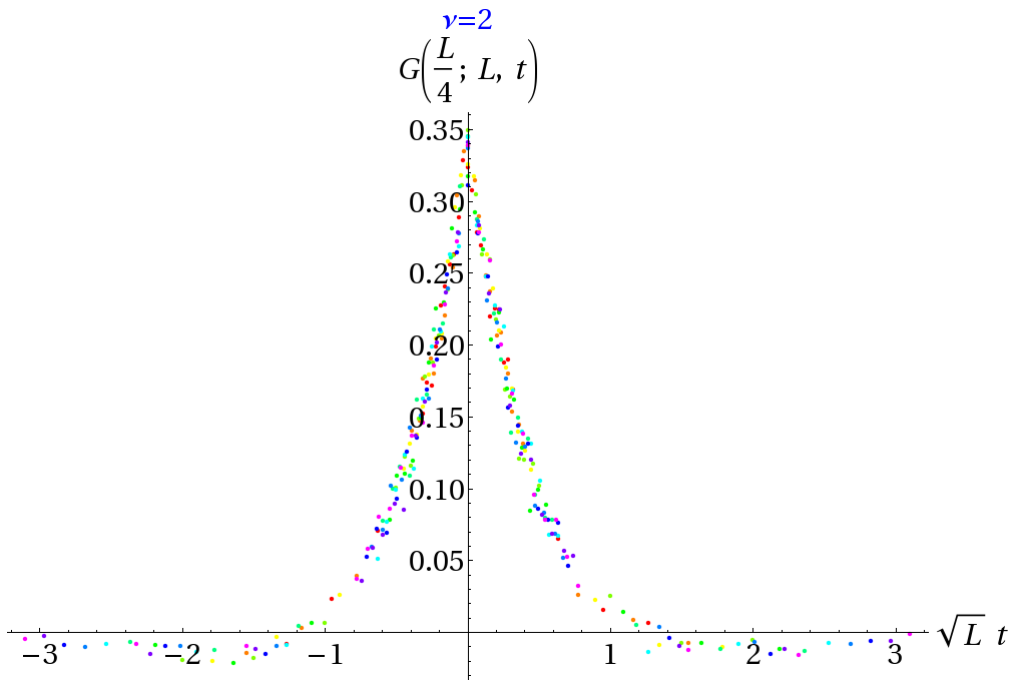


Figure 5: The correlation function from different values of  $L$  at  $t$  at  $r/L = 1/4$  as a function of  $\sqrt{L}t$ .

$p$	$-\alpha$
1	$0.00 \pm 0.03$
0.95	$0.08 \pm 0.04$
0.90	$0.18 \pm 0.04$
0.85	$0.28 \pm 0.04$
0.80	$0.37 \pm 0.04$
0.75	$0.47 \pm 0.04$

Table 1: Numerical estimates of the critical exponent  $\alpha$  in the region  $p < 1$ .

## 2.2 Analytical predictions at criticality

Because of the presence of a critical point we can define the model in the continuum limit, where, in the rescaled coordinate, the process  $\varphi_i$  becomes  $\varphi(s)$  with a *time* variable  $s \in [0, 1]$ . Indeed, for  $i = 1, \dots, L$

$$\varphi_i = b_i - i + \frac{1}{2}. \quad (30)$$

The probability to find the  $i$ -th blue point in the interval  $[y, y + dy]$ , when there are  $L$  blue points in the interval  $[0, L]$ , is given by

$$P_i(dy) = \frac{\frac{y^{i-1}}{(i-1)!} \frac{(L-y)^{L-i}}{(L-i)!}}{\frac{y^L}{L!}} dy = \binom{L}{i} \left(\frac{y}{L}\right)^i \left(1 - \frac{y}{L}\right)^{L-i} \frac{i}{y} dy = B_i\left(L; \frac{y}{L}\right) \frac{i}{y} dy \quad (31)$$

where  $B_i(n; p)$  is the binomial distribution for a process with  $n$  independent yes or no experiments, each with probability  $p$  of success, so that in the limit of large  $L$ , by keeping fixed the ratio  $y/L$ , we get, by the central limit theorem, that

$$B_i\left(L; \frac{y}{L}\right) \rightarrow \frac{e^{-\frac{(i-y)^2}{2L\frac{y}{L}\left(1-\frac{y}{L}\right)}}}{\sqrt{2\pi L\frac{y}{L}\left(1-\frac{y}{L}\right)}} \quad (32)$$

which tells us that the difference  $i - y$  is of order  $\sqrt{L}$  so that by the change of variables

$$\varphi_i = \sqrt{L} x_i + \frac{1}{2} \quad (33)$$

we get the probability distribution

$$p_{B(s)}(x) = \frac{e^{-\frac{x^2}{2s(1-s)}}}{\sqrt{2\pi s(1-s)}} \quad (34)$$

with  $s = y/L$ , which is the Gaussian probability distribution of a Brownian bridge  $B(s)$  over the interval  $[0, 1]$  (see Fig. 6). The interested reader can find all the necessary definitions in Appendix A. Essentially the same calculation can be performed for the joint probability distribution for displacements from different blue points to see that it always provides, in the limit of large  $L$ , the joint distribution at different times of a Brownian bridge.

Remark that this result would remain unchanged for the Poisson-Poisson matching. In that case, also the red points would be distributed like the blue points, and the difference of two random variables distributed according to the same binomial distribution  $B(L; y/L)$  is still a binomial with distribution  $B(2L; y/L)$ . In order to converge to the same continuum limit we must rescale

$$\varphi_i = \sqrt{2L} x_i. \quad (35)$$

As a first consequence of the distribution function that we have obtained, we

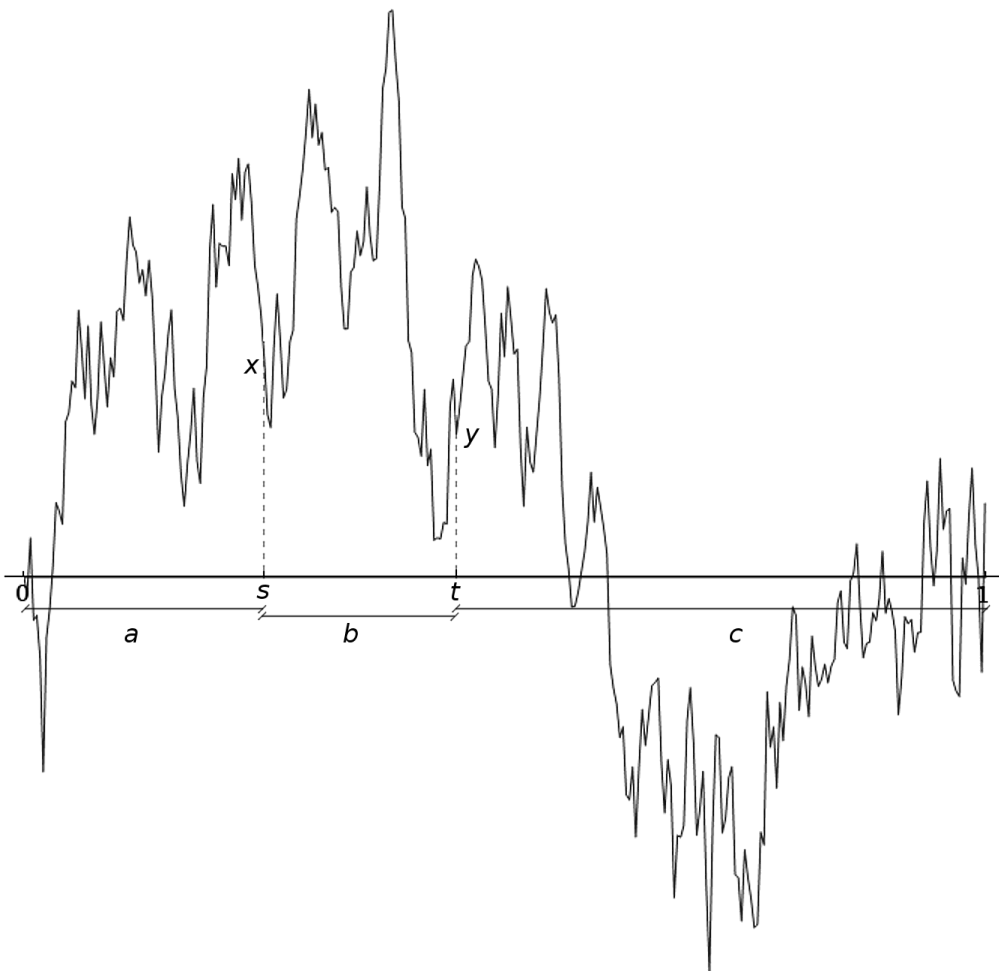


Figure 6: An example of Brownian bridge  $B$  over the interval  $[0, 1]$  with intermediate times  $s$  and  $t$

can evaluate the cost of the optimal Grid-Poisson matching:

$$L^{-\frac{p}{2}} E_{opt} \rightarrow \int_0^1 ds \mathbb{E}(x^p(s)) = \int_0^1 ds \frac{[2s(1-s)]^{\frac{p}{2}}}{\sqrt{\pi}} \Gamma\left(\frac{1+p}{2}\right) \quad (36)$$

$$= \sqrt{\frac{2^p}{\pi}} \frac{\Gamma^2\left(\frac{p}{2} + 1\right)}{\Gamma(p+2)} \Gamma\left(\frac{1+p}{2}\right) \quad (37)$$

$$= \sqrt{\frac{2^{-p}}{\pi}} \frac{\Gamma\left(\frac{p}{2} + 1\right)}{p+1} \quad (38)$$

for  $p > 1$ , so that, in particular, for  $p = 2$  we get

$$L^{-1} E_{opt} \rightarrow \int_0^1 ds s(1-s) = \frac{1}{6}. \quad (39)$$

Now, let us consider two intermediate times,  $s$  and  $t$ , with  $0 < s < t < 1$ . The probability that the process started at the origin arrives at  $x_1$  after a time  $s$  is that of a Wiener process, so that it is a Gaussian with zero mean and variance  $s$ :

$$p_{W(s)}(x_1) = \frac{1}{\sqrt{2\pi s}} e^{-\frac{x_1^2}{2s}}. \quad (40)$$

Similarly, to move from  $x_1$  to  $x_2$  in the interval  $(t-s)$ :

$$p_{W(t-s)}(x_2 - x_1) = \frac{1}{\sqrt{2\pi(t-s)}} e^{-\frac{(x_2-x_1)^2}{2(t-s)}} \quad (41)$$

and, finally, to move from  $x_2$  to 0 in the interval  $(1-t)$ :

$$p_{W(1-t)}(x_2) = \frac{1}{\sqrt{2\pi(1-t)}} e^{-\frac{x_2^2}{2(1-t)}}. \quad (42)$$

Since the distribution is Gaussian, which means that the joint distribution has the form (103)

$$p_A(x_1, x_2) = \sqrt{\det A} \frac{e^{-\frac{1}{2} \sum_{i=1}^2 x_i A_{ij} x_j}}{2\pi}, \quad (43)$$

by a change of parameters, if we consider the three segments of length

$$\begin{aligned} a &= s \\ b &= t - s \\ c &= 1 - t, \end{aligned} \quad (44)$$

we get that the matrix  $A$  is given by

$$A = \begin{pmatrix} \frac{1}{a} + \frac{1}{b} & -\frac{1}{b} \\ -\frac{1}{b} & \frac{1}{c} + \frac{1}{b} \end{pmatrix}. \quad (45)$$

with

$$\det A = \frac{a+b+c}{abc}. \quad (46)$$

### 2.2.1 Correlation function

Given the continuous variable

$$\sigma(s) := \frac{\varphi(s)}{|\varphi(s)|} = \text{sgn}(\varphi(s)) \quad (47)$$

for  $s \in [0, 1]$ , we shall look at the correlation function

$$G_1(s, t) = \sigma(s)\sigma(t) = \text{sgn}(\varphi(s)\varphi(t)). \quad (48)$$

Therefore, the quantity we want to calculate is

$$\begin{aligned} G_2(a, b, c) &= \int \int dx dy p_A(x, y) \text{sgn}(x \cdot y) \\ &= \int \int dx dy \sqrt{2\pi} \sqrt{a+b+c} \frac{e^{-\frac{x^2}{2a} - \frac{(x-y)^2}{2b} - \frac{y^2}{2c}}}{\sqrt{2\pi a} \sqrt{2\pi b} \sqrt{2\pi c}} \text{sgn}(x \cdot y) \end{aligned} \quad (49)$$

If we define

$$\alpha(a, b, c) := \int_{x \geq 0} \int_{y \geq 0} dx dy p_A(x, y) \quad (50)$$

and

$$\beta(a, b, c) := \int_{x \geq 0} \int_{y \leq 0} dx dy p_A(x, y), \quad (51)$$

then

$$G_2(a, b, c) = 2\alpha(a, b, c) - 2\beta(a, b, c). \quad (52)$$

In addition, since  $p_A(x, y)$  is Gaussian, we know that

$$2\alpha(a, b, c) + 2\beta(a, b, c) = 1, \quad (53)$$

then

$$G_2(a, b, c) = 4\alpha(a, b, c) - 1. \quad (54)$$

By performing the integral (50), we find

$$\alpha(a, b, c) = \frac{1}{4} + \frac{1}{2\pi} \arctan \sqrt{\frac{ac}{b(a+b+c)}}, \quad (55)$$

and then

$$G_2(a, b, c) = \frac{2}{\pi} \arctan \sqrt{\frac{ac}{b(a+b+c)}}, \quad (56)$$

with, in this case,

$$\begin{aligned} a, b, c &\geq 0 \\ a + b + c &= 1. \end{aligned} \quad (57)$$

If we keep the distance  $b$  between the two points constant, and we calculate the mean over the interval  $[0, 1]$ , we finally obtain

$$\hat{G}_{obc}(b) = \frac{2}{\pi} \frac{1}{1-b} \int_0^{1-b} da \arctan \sqrt{\frac{a(1-a-b)}{b}} = \frac{1-\sqrt{b}}{1+\sqrt{b}}. \quad (58)$$

We found an excellent agreement of the theoretical predictions with the numerical data, even at sizes as small as  $L = 100$ . This can be seen in Fig. 3.

### 3 Periodic boundary conditions

We shall now study the same problem by taking periodic boundary conditions, that is, instead of being on a line we are on a circle.

#### 3.1 Numerical results

In Fig. 7 we report the correlation function  $G(r; L, t)$  for various choices of the parameter  $t$  when the size of the system is  $L = 6000$ . Each curve is the mean over  $10^3$  instances. The function is even under the parity  $r \rightarrow L - r$  so that we plot it only in the interval  $[0, L/2]$ . The function  $G(r; L, t)$  still presents two ranges of behaviour. If  $|t| < \bar{t}(L)$ , with  $\bar{t}(6000) \approx 0.01$ , the function is decreasing with  $r$ , and has, therefore, a minimum at  $r = \frac{L}{2}$ . But it is no longer positive definite. When  $|t| > \bar{t}(L)$ , the shape is different. It reaches a minimum at an intermediate value  $r'$ , then goes up again approaching zero as  $r \rightarrow \frac{L}{2}$ .

In Fig. 8 we show the correlation functions at criticality for various sizes. Each numerical point has been obtained by using  $10^4$  instances for the positions of the blue points. Again, all curves are trivially mapped one onto the others by the simple rescaling  $r \rightarrow r/L$ .

When  $|t| < \bar{t}(L)$ , if we define  $\bar{x}_L$  as the point where the curve for the size  $L$  has a zero, we find that  $\bar{x}_L(t)$  has a maximum at criticality  $t = 0$  (see Fig. 9). The value of  $\bar{x}_L/L$  at criticality as a function of the size  $L$  is almost constant, we get

$$\frac{\bar{x}_L(t=0)}{L} \approx 0.2117 \pm 0.0004. \quad (59)$$

#### 3.2 Analytical predictions at criticality

In the problem with periodic boundary conditions, at criticality, we still have two sets of points with the same cardinality. Now the ordering of points is more subtle. First of all we need to consider triple of points. The following lemma is what we

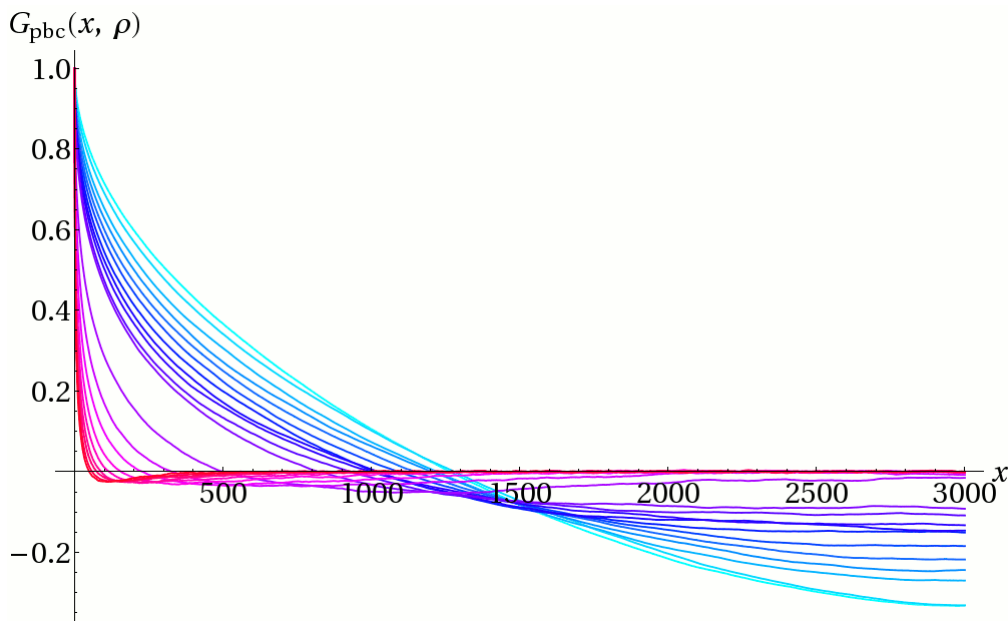


Figure 7: The correlation function near the critical point at size 6000 with periodic boundary conditions. From cyan to purple,  $t = 0, 0.001, 0.002, 0.003, 0.004, 0.005, 0.006, 0.007, 0.008, 0.009, 0.01, 0.02, 0.03, 0.04, 0.05, 0.06, 0.07, 0.08, 0.09, 0.1$ .

need to obtain a complete characterization of the solution for the matching problem at least when  $p \geq 1$ .

**Proposition 3.1** *Consider the matching problem for points on the circle of unit length  $\mathcal{S}^1$  with distance between two points as the minimal length along the two possible connecting paths. There exists an optimal matching  $\pi$  such that for all triples  $(i, j, k)$  of red points counter-clockwise ordered in  $\mathcal{S}^1$ , the triple  $(\pi(i), \pi(j), \pi(k))$  is counter-clockwise ordered.*

**Proof.** Consider the positions  $r_i, r_j, r_k$  of the given three red points, the positions of the the blue points  $b_{\pi(i)}, b_{\pi(j)}, b_{\pi(k)}$  and the positions of their antipodal points. This makes 12 points on  $\mathcal{S}^1$  and 12 intervals, each one of equal length with its opposite. Let us fix, without loss of generality, that  $r_1 = 0$  and let us relabel red and blue points, and intervals, in counter-clockwise order starting from it. All intervals  $a_i$  are assumed to be of positive length. The distance between the red and blue points is easily determined as, for each couple, the two options are of the form  $a_l + \dots + a_{l+s}$  and  $a_l + a_{l+s} + 2a_{l+s+1} + \dots + 2a_{l+6}$  where all the indices are modulo 6, for  $1 \leq s \leq 6$  and  $1 \leq l \leq 6$ . There exists  $2^5 \binom{5}{2} = 320$  possible patterns. We checked, by computer, the existence of the claimed optimal matching.  $\square$

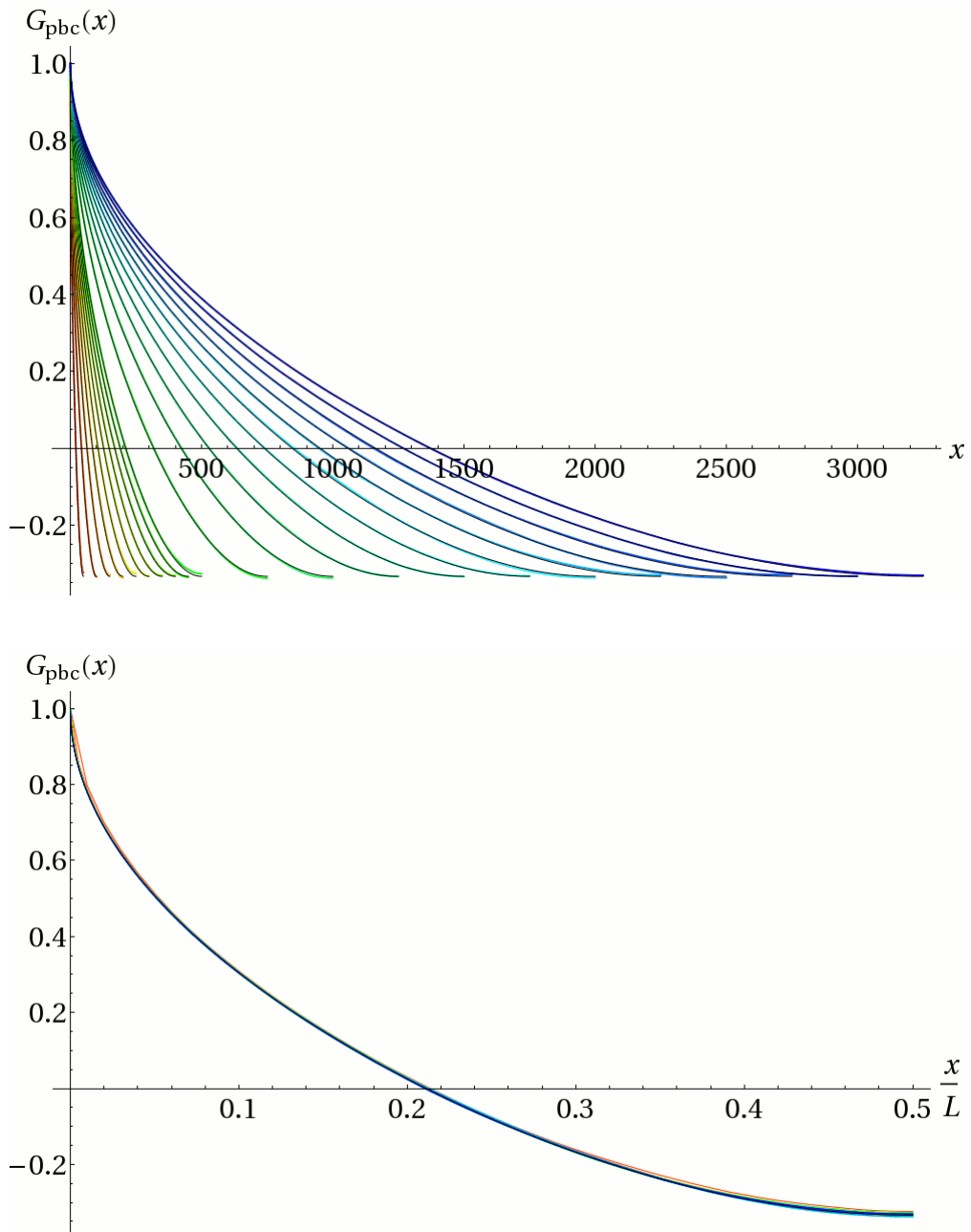


Figure 8: The correlation function with periodic boundary conditions at the critical point. Top: increasing sizes are represented from red ( $L = 100$ ) to blue ( $L = 6500$ ); Bottom: the same experimental curves, rescaled to show the agreement with the theoretical function, regardless of the size.

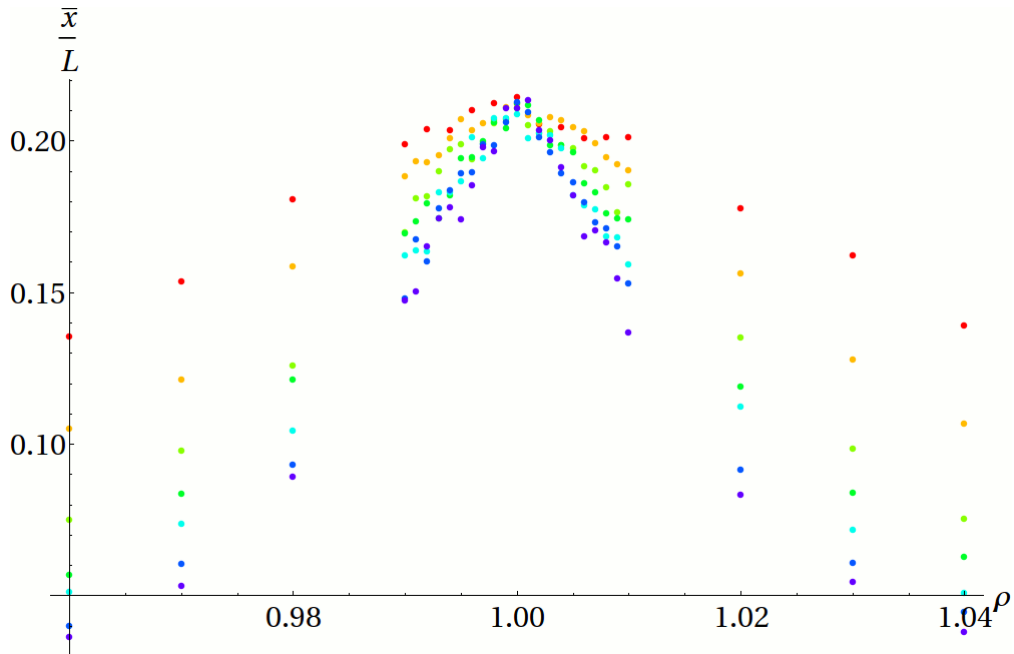


Figure 9: The experimental rescaled intersection with the  $x$ -axis ( $\bar{x}_L/L$ ) as a function of the *reduced temperature*  $t$ . Colours from red to purple for sizes  $L = 500, 1000, 2000, 3000, 4000, 5000, 6000$ .

**Proposition 3.2** *Let  $R$  be the permutation  $(2\ 3\ 4\ \dots\ L-1)$ . All the permutations satisfying the previous Proposition are those of the form  $R^l$  with  $l = 0, \dots, L-1$ .*

**Proof.** Let  $i \neq j$ . Either  $\pi(i) - \pi(j) = i - j$  modulo  $L$  for all pairs, or there exists at least a couple of indices  $i$  and  $j$  such that  $\pi(i) - \pi(j) \neq i - j$  modulo  $L$ . In this case consider the interval  $I = (i, i+1, \dots, j)$  and  $J = (\pi(i), \pi(i)+1, \dots, \pi(j))$  where all the sums are modulo  $L$ . As these intervals have different cardinality, there must exist a  $k$  such that either  $k \in I$  and  $\pi(k) \notin J$  or  $k \notin I$  and  $\pi(k) \in J$ . Therefore  $\pi$  has a negative signature on the triple  $(i, j, k)$ .  $\square$

This means that, after the relabelling of the indices of the indices of both sets  $\mathcal{R}$  and  $\mathcal{B}$  in increasing counter-clockwise order, the solution of the matching problem will have the form

$$\varphi_i = b_i - r_{i+l} \tag{60}$$

with a particular  $l \in \{0, \dots, L-1\}$  and  $i+l$  has to be taken modulo  $L$ .

In the continuum limit, after the rescaling with  $L$ , the integer shift  $l$  will become a real variable  $\lambda \in [0, 1]$ . Then we can still represent our process with a Brownian

bridge, but this time the first point is not mapped to zero, but to some constant  $\lambda$ . That is

$$\varphi_\lambda(s) = B(s) + \lambda \quad (61)$$

whose cost is

$$E[\varphi_\lambda] = \int_0^1 ds |\varphi_\lambda(s)|^p = \int_0^1 ds |B(s) + \lambda|^p, \quad (62)$$

and the optimality condition

$$\frac{d}{d\lambda} E[\varphi_\lambda] = p \int_0^1 ds \frac{|\varphi_\lambda(s)|^p}{\varphi_\lambda(s)} = 0 \quad (63)$$

provides a linear relation on the process  $B(s)$  only when the cost function is taken to be the square of the distance, that is the exponent  $p$  is chosen to be  $p = 2$ . Indeed in this case the optimality condition is solved by choosing the shift according to

$$\lambda = - \int_0^1 ds B(s) \quad (64)$$

where, on the right-hand-side we have the area under the path after time  $t$

$$B^{(-1)}(t) := \int_0^t ds B(s) \quad (65)$$

evaluated at the final time  $t = 1$ .

We therefore take as our solution

$$\varphi(s) = B(s) - B^{(-1)}(1) \quad (66)$$

which is still linear in the process  $B(s)$ . This is, again, a Gaussian random variable with zero expectation value. Its covariance can be easily calculated as follows:

$$\text{cov}[B(s) - B^{(-1)}(1), B(t) - B^{(-1)}(1)] = \frac{1}{12} - \frac{1}{2}t(1-t) - \frac{1}{2}s(1-s) + \min(s, t) - st. \quad (67)$$

If we assume  $s \leq t$ , this expression becomes

$$\text{cov}[\varphi(s), \varphi(t)] = \frac{1}{12} - \frac{1}{2}(t-s)(1-(t-s)), \quad (68)$$

which, as we could expect, is no longer a function of  $s$  and  $t$  separately, but rather of their difference, and depends symmetrically on  $t-s$  and  $1-(t-s)$ . And this satisfies

$$\frac{d^2}{ds^2} \text{cov}[\varphi(s), \varphi(t)] = -\delta(s-t) + 1 \quad (69)$$

where the correction to the  $\delta$ -function is necessary because on a compact without boundaries the integral of the left-hand side on the whole interval vanishes.

As a consequence, with periodic boundary conditions, the optimal cost for unit length is

$$L^{-1}E_{opt} = \frac{1}{12} \quad (70)$$

in agreement with the analysis performed in [16] for the Poisson-Poisson matching which must differ from this result of a factor two.

If we define

$$\tau = t - s \quad (71)$$

and

$$\lambda = \tau(1 - \tau) = (t - s)(1 - (t - s)), \quad (72)$$

the covariance matrix can be written as

$$C = \begin{pmatrix} \frac{1}{12} & \frac{1}{12} - \frac{1}{2}\lambda \\ \frac{1}{12} - \frac{1}{2}\lambda & \frac{1}{12} \end{pmatrix} \quad (73)$$

and therefore in this case the joint probability distribution is still of the form (103), now with the matrix  $A$

$$A = C^{-1} = \frac{1}{\lambda(1 - 3\lambda)} \begin{pmatrix} 1 & -1 + 6\lambda \\ -1 + 6\lambda & 1 \end{pmatrix}. \quad (74)$$

By comparing (45) with (74), we find

$$\begin{aligned} b &= \frac{\lambda(1-3\lambda)}{1-6\lambda} \\ a = c &= \frac{1-3\lambda}{6}. \end{aligned} \quad (75)$$

The important difference with respect to the non-periodic case is that

$$a + b + c = \frac{(1 - 3\lambda)^2}{3(1 - 6\lambda)}, \quad (76)$$

which is in general  $\neq 1$ . Moreover,  $b$  and  $a + b + c$  can now have a negative sign:

$$\begin{aligned} b &< 0 \\ a + b + c &< 0 \end{aligned} \quad \text{if } \lambda > \frac{1}{6}. \quad (77)$$

If  $\lambda < \frac{1}{6}$ , the result in (55) is still valid, while if  $\lambda > \frac{1}{6}$ , we obtain<sup>1</sup>

$$\alpha(a, b, c) = \frac{1}{2\pi} \arctan \sqrt{\frac{b(a + b + c)}{ac}} \quad (78)$$

$$= \frac{1}{2\pi} \left[ \arctan \left( -\sqrt{\frac{ac}{b(a + b + c)}} \right) + \frac{\pi}{2} \right], \quad (79)$$

---

<sup>1</sup>Here we have used the trigonometric identities:  $\arctan x + \arctan(\frac{1}{x}) = \frac{\pi}{2}$  and  $\arctan(-x) = -\arctan x$ .

which leads to

$$G_3(\lambda) = \begin{cases} \frac{2}{\pi} \arctan\left(\frac{|1-6\lambda|}{\sqrt{12\lambda(1-3\lambda)}}\right) & \text{if } \lambda < \frac{1}{6} \\ \frac{2}{\pi} \arctan\left(-\frac{|1-6\lambda|}{\sqrt{12\lambda(1-3\lambda)}}\right) & \text{if } \lambda > \frac{1}{6} \end{cases} \\ = \frac{2}{\pi} \arctan\left(\frac{1-6\lambda}{\sqrt{12\lambda(1-3\lambda)}}\right). \quad (80)$$

Or, as a function of  $\tau$ ,

$$\hat{G}_{pbc}(\tau) = \frac{2}{\pi} \arctan\left(\frac{1-6\tau(1-\tau)}{\sqrt{12\tau(1-\tau)(1-3\tau(1-\tau))}}\right). \quad (81)$$

Once more we find an excellent agreement with the numerical data, even at sizes as small as  $L = 100$ . This can be seen in Fig. 8.

From the analytic expression (81), we see that the correlation function vanishes when

$$1 - 6\tau(1 - \tau) = 0 \quad (82)$$

that is when

$$\bar{\tau} = \frac{1}{6} (3 - \sqrt{3}) \quad (83)$$

which numerically coincides with the value given in (59), and, of course, in  $1 - \bar{\tau}$ .

### 3.3 Comparison for different weight functions

We have also considered what happens when we change the exponent  $p$  which appears in the cost function, by looking also at the values  $p = 1, 3, 4$ . In these cases we have seen that the shift which determines the optimal solution is, in general, different from what we could get at  $p = 2$ . We see that these differences are really tiny.

In Fig. 10 we show the correlation function at criticality, that is  $t = 0$ , for the size  $L = 5000$ . Each curve is the mean over  $10^3$  instances.

## 4 Conclusions

We studied the Euclidean bipartite matching problem of points on a grid with points chosen at random when the cost is a power  $p$  of the distance.

At criticality, that is when the two set of points have the same cardinality, we can solve exactly the case of open boundary conditions for all  $p > 1$  and, the

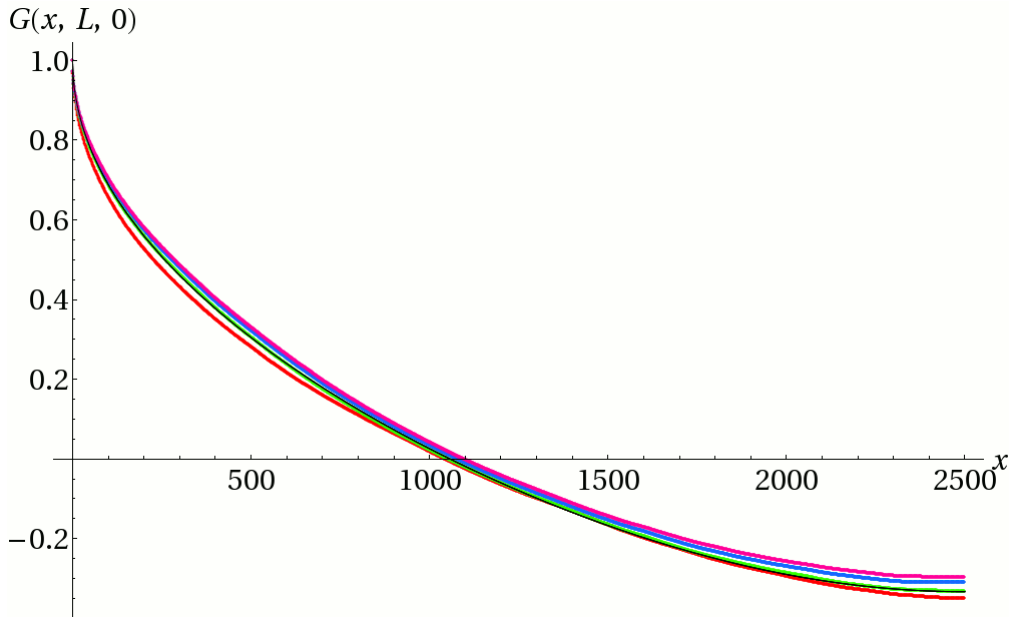


Figure 10: Comparison of the correlation function at criticality, with different values of  $p$  ( $L = 5000$ ). From red to purple,  $p = 1, 2, 3, 4$  (green is  $p = 2$ ). The black thinner curve is the plot of the analytic function which is valid only for the case  $p = 2$ .

case of periodic boundary conditions, only when  $p = 2$ . Different values of the parameter  $p$  and the case of different number of points in the two sets have been studied numerically.

We have computed the average cost and the two-point correlation function averaged on the distribution of random points. We have verified by a finite-size scaling analysis the existence of a nontrivial continuum limit in which the number of the two set of points is equal and sent to infinity. In this limit a strict relation with the Brownian bridge process emerges.

In the exactly soluble models we find the values  $\nu = 2$  and  $\alpha = 0$  for the critical exponents which governs the scaling (11).

It would be interesting to understand the tiny changes in the two-point correlation function with  $p > 1$  in the case of periodic boundary conditions.

## Acknowledgements

It is a pleasure to thank Massimiliano Gubinelli for very useful discussions on the continuum limit and Davide Fichera on the Hungarian Algorithm.

# A Wiener process and Brownian bridges

## A.1 Wiener process

A standard one-dimensional *Wiener process*, or *Brownian motion process*, is a stochastic process  $W(t)$ :  $t \in \mathbb{R}$ ,  $t \geq 0$ , with the following properties:

- (1)  $W(0) = 0$
- (2) The function  $t \rightarrow W(t)$  is almost surely continuous
- (3) The process  $W(t)$  has stationary, independent increments
- (4) The increment  $W(t) - W(s)$  is normally distributed with expected value 0 and variance  $t - s$

The requirement that  $W(t)$  have *independent increments* means that for all  $t_0 < t_1 < \dots < t_n$ , the  $n$  random variables  $W(t_1) - W(t_0)$ ,  $W(t_2) - W(t_1)$ ,  $\dots$ ,  $W(t_n) - W(t_{n-1})$  are independent. The increments are further said to be *stationary* if, for any  $t > s$  and  $h > 0$ , the distribution of  $W(t+h) - W(s+h)$  is the same as the distribution of  $W(t) - W(s)$ .

## A.2 Basic properties of the Wiener process

- $W(t)$  is a *Gaussian process*, that is for all  $n$  and times  $t_1, \dots, t_n$ , linear combinations of  $W(t_1), \dots, W(t_n)$  are normally distributed
- The unconditional probability density function at a fixed time  $t$  is given by

$$p_{W(t)}(x) = \frac{1}{\sqrt{2\pi t}} e^{-\frac{x^2}{2t}} \quad (84)$$

- $\forall t$ , the expectation is zero:

$$\mathbb{E}[W(t)] = 0 \quad (85)$$

- The variance:

$$\text{var}[W(t)] = \mathbb{E}[W^2(t)] - \mathbb{E}^2[W(t)] = \mathbb{E}[W^2(t)] = t \quad (86)$$

- The covariance<sup>2</sup>:

$$\text{cov}[W(s), W(t)] = \min(s, t) \quad (87)$$

The area of a Gaussian process, defined by

$$W^{(-1)}(t) := \int_0^t ds W(s), \quad (88)$$

is itself a Gaussian process (as a linear combination of Gaussian processes) characterized by its expected value and variance:

$$\mathbb{E}[W^{(-1)}(t)] = \int_0^t ds \mathbb{E}[W(s)] = 0 \quad (89)$$

$$\begin{aligned} \text{var}[W^{(-1)}(t)] &= \mathbb{E} \left[ \int_0^t ds \int_0^t ds' W(s)W(s') \right] = \int_0^t ds \int_0^t ds' \text{cov}(W_s, W_{s'}) \\ &= \int_0^t ds \left( \int_0^s ds' \min(s, s') + \int_s^t ds' \min(s, s') \right) = \frac{t^3}{3}. \end{aligned} \quad (90)$$

### A.3 Brownian bridge

A standard *Brownian bridge*  $B(t)$  over the interval  $[0, 1]$  is a standard Wiener process conditioned to have  $B(1) = B(0) = 0$ .

Now, if we have a Wiener process  $W(t)$ , the linear combination

$$B(t) := W(t) - tW(1) \quad (91)$$

is a Brownian bridge with expectation, variance and covariance:

$$\mathbb{E}[B(t)] = 0 \quad (92)$$

$$\begin{aligned} \text{var}[B(t)] &= \mathbb{E}[(W(t) - tW(1))^2] \\ &= \mathbb{E}[W^2(t)] - 2t \mathbb{E}[W(1) \cdot W(t)] + t^2 \mathbb{E}[W^2(1)] \\ &= t(1 - t) \end{aligned} \quad (93)$$

---

<sup>2</sup>To see this, let us suppose  $s \leq t$ . Then

$$\begin{aligned} \text{cov}[W(s), W(t)] &= \mathbb{E}[(W(s) - \mathbb{E}[W(s)]) \cdot (W(t) - \mathbb{E}[W(t)])] \\ &= \mathbb{E}[W(s) \cdot W(t)] = \mathbb{E}[W(s) \cdot ((W(t) - W(s)) + W(s))] \\ &= \mathbb{E}[W(s) \cdot (W(t) - W(s))] + \mathbb{E}[W^2(s)] = s \end{aligned}$$

$$\begin{aligned}\text{cov}[B(s), B(t)] &= \mathbb{E}[(W(s) - sW(1)) \cdot (W(t) - tW(1))] \\ &= \min(s, t) - st.\end{aligned}\tag{94}$$

This covariance is the Green's function of the second derivative with the given boundary conditions. Indeed,

$$\frac{d^2}{ds^2} \text{cov}[B(s), B(t)] = -\delta(s - t)\tag{95}$$

and this means that the weight of a configuration is

$$W[B] = \exp \left[ - \int_0^1 ds \left( \frac{dB}{ds} \right)^2 \right].\tag{96}$$

The area of a Brownian bridge, defined by

$$B^{(-1)}(t) := \int_0^t ds B(s),\tag{97}$$

is, again, a Gaussian variable (as a linear combination of Gaussian random variables) characterized by its expected value and variance:

$$\mathbb{E}[B^{(-1)}(t)] = \int_0^t ds \mathbb{E}[B(s)] = 0\tag{98}$$

$$\begin{aligned}\text{var}[B^{(-1)}(t)] &= \int_0^t ds \int_0^t ds' \text{cov}[B(s), B(s')] \\ &= \int_0^t ds \int_0^t ds' (\min(s, s') - s s') \\ &= \frac{t^3}{3} - \frac{t^4}{4}.\end{aligned}\tag{99}$$

In particular, if  $t = 1$ ,

$$\text{var}[B^{(-1)}(1)] = \frac{1}{12}\tag{100}$$

and the covariance between  $B^{(-1)}(1)$  and  $B(t)$  is

$$\begin{aligned}\text{cov}[B^{(-1)}(1), B(t)] &= \int_0^1 ds \text{cov}[B(s), B(t)] = \int_0^1 ds (\min(s, t) - st) \\ &= \frac{1}{2} t (1 - t).\end{aligned}\tag{101}$$

Let us consider Brownian bridge  $B$  at two different times,  $B(s)$  and  $B(t)$ , and let us assume that  $s \leq t$ . The covariance matrix is then

$$C = \begin{pmatrix} s(1-s) & s(1-t) \\ s(1-t) & t(1-t) \end{pmatrix}. \quad (102)$$

The distribution is Gaussian, which means the density function is given by

$$p_A(x_1, x_2) = \sqrt{\det A} \frac{e^{-\frac{1}{2} \sum_{i=1}^2 x_i A_{ij} x_j}}{2\pi}, \quad (103)$$

with (see, for example, [20])

$$A = C^{-1} = \begin{pmatrix} \frac{t}{s(t-s)} & -\frac{1}{t-s} \\ -\frac{1}{t-s} & \frac{1-s}{(1-t)(t-s)} \end{pmatrix} \quad (104)$$

## References

- [1] Gaspard Monge, *Mémoire sur la théorie des déblais et des remblais*, in *Histoire de l'Académie Royale des Sciences, Année MDCCLXXXI. Avec les Mémoires de Mathématiques et de Physique pour la même année*, Paris, 1784.
- [2] C. Villani, *Optimal Transport: Old and New*, Grundlehren der Mathematischen Wissenschaften, Springer, 2008.
- [3] H. Kuhn, *The Hungarian Method for the assignment problem*, Naval Research Logistics Quarterly 2, 83–97, 1955.
- [4] D. E. Knuth, *The Stanford GraphBase: A Platform for the Combinatorial computing*, Addison-Wesley, 1993.
- [5] J. Munkres, *Algorithms for the Assignment and Transportation Problems*, J. Soc. Ind. and Appl. Math. 5, 32–38, 1957.
- [6] M. Mézard, G. Parisi, M. A. Virasoro, *Spin Glass Theory and Beyond*, World Scientific, Singapore, 1987.
- [7] A. K. Hartmann, M. Weigt, *Phase Transitions in Combinatorial Optimization Problems*, John Wiley & Sons, 2006.
- [8] A. Percus, G. Istrate, C. Moore, *Computational Complexity and Statistical Physics*, Oxford University Press, 2006.
- [9] *Complex Systems: Lecture Notes of the Les Houches Summer School 2006*, J.-P. Bouchaud, M. Mézard, J. Dalibard, eds., Elsevier, 2007.

- [10] M. Mézard, A. Montanari, *Information, Physics, and Computation*, Oxford University Press, 2009.
- [11] M. Mézard, G. Parisi, *Mean-Field Equations for the Matching and the Travelling Salesman Problem*, Europhys. Lett. 2, 913–918, 1986.
- [12] M. Mézard, G. Parisi, *On the solution of the random link matching problem*, J. Physique 48, 1451–1459, 1987.
- [13] D. J. Aldous, *The  $\zeta(2)$  limit in the random assignment problem*, Random Structures and Algorithms 18, 381–418, 2001.
- [14] M. Ajtai, J. Komlós and G. Tusnády, *On optimal matchings*, Combinatorica 4, 259–264, 1984.
- [15] A. Holroyd, R. Pemantle, Y. Peres, O. Schramm, *Poisson Matching*, Ann. Inst. Henri Poincaré Probab. Stat. 45, 266–287, 2009 (arXiv:0712.1867).
- [16] S. Caracciolo, C. Lucibello, G. Parisi, G. Sicuro, *A Scaling Hypothesis for the Euclidean Bipartite Matching Problem*, (arXiv:1402.6993).
- [17] M. Mézard, G. Parisi, *The Euclidean matching problem*, J. Physique 49, 2019–2015, 1988.
- [18] T. Leighton and P. Shor, *Tight bounds for minimax grid matching with applications to the average case analysis of algorithms*, Combinatorica 9, 161–187, 1989.
- [19] P. W. Shor and J. E. Yukich, *Minimax grid matching and empirical measures*, Ann. Prob. 19, 1338–1348, 1991.
- [20] R. Durrett, *Probability: Theory and Examples*, 4th Edition, Cambridge University Press, 2010.